

# Computational Simulation of Ultraviolet ZnO Diode Laser

**A.Ouerdane<sup>1,2</sup>, M.Bousslama<sup>2</sup>, A. Abdellaoui<sup>2</sup>, M.Ghaffour<sup>2</sup> and Y. Al Douri<sup>3</sup>**

<sup>1</sup> Centre Universitaire Khemis Miliana route de Theniet El Had 44225 Ain Defla, Algeria

<sup>2</sup>Laboratoire Matériaux ENSET Mnaouer BP 1523 Oran 31000 , Algeria

<sup>3</sup> Institute of Nanoelectronic Engineering, University Malaysia Perlis, Malaysia

Email : [ouerdanea@yahoo.fr](mailto:ouerdanea@yahoo.fr)

**Abstract:** This article deals with a mathematical technique for the study of functionality of semiconductor laser, by its rate equations, to be used in the simulation of high speed optical systems. We describe the development of numerical simulation model of a p-ZnO laser emitting in UV optical wavelength. A powerful dynamic algorithmical model is used to study the p-ZnO active region waveguide laser. It is based on time dependant rate equations of a quasi two levels system for the population density and time dependant for the pump and optical signal power. The model is sufficient to account for many of the observed dynamics in a single mode semiconductor laser in response to a dynamic drive current, such as relaxation oscillations and frequency chirping.

## 1. Introduction

Recently one can observe a great interest to ZnO films possessing nanocrystallites as materials for electronics, optoelectronics and others technological applications. With a wide band gap which is equal at 3.37 eV and a resistivity ( $10^{-5}$  - $10^{-3}$   $\Omega$  cm) which comes, partly, from stoichiometric shift mainly due to oxygen vacancies and/or zinc interstitials, ZnO is a good materials for ultra violet diode laser (LD) which are widely used for applications in photonics, information storage, biology and medical therapeutics[1,2].

The optical power emitted by the diode laser is proportional to the current supplied to the ZnO semiconductor heterojunction. The laser dynamics can be modeled by coupled rate equations which describe the relation between the carrier number, the photon density and the optical phase[3]. To use these models, values for the rate equations, parameters must be chosen appropriately in order to obtain agreement between simulated and measured results for system performance.

The purpose of this work is to solve the coupled nonlinear rate equations describing the complex electric field and the carrier density in a simple model of the ZnO semiconductor laser. The model is sufficient to account for many of the observed dynamics in a single mode semiconductor laser in response to a dynamic drive current, such as relaxation oscillations and frequency chirping [4].

---

<sup>1</sup> To whom any correspondence should be addressed



The output of the solver is the time, injection current, and the transformed components of the state vector, computed at discrete time steps. The rate equations are integrated using the fourth order Runge-Kutta computation [5]

## 2. Rate equations: steady state

The laser dynamics can be modeled by coupled rate equations which describe the relation between the carrier number  $N_p(t)$ , the photon density  $S_p(t)$  and the optical phase  $\varphi(t)$ . [1-6].

$$\frac{dN_p(t)}{dt} = \frac{I(t)}{q} - \frac{N_p(t)}{\tau_n} - g(N, T) \frac{N_p(t) - N_0}{1 + \varepsilon S_p(t)} S_p(t) \quad (1)$$

$$\frac{dS_p(t)}{dt} = \Gamma g(N, T) \frac{N_p(t) - N_0}{1 + \varepsilon S_p(t)} S_p(t) - \frac{S_p(t)}{\tau_p} + \Gamma \frac{\beta N_p(t)}{\tau_n} \quad (2)$$

$$\frac{d\varphi(t)}{dt} = \frac{\alpha_0}{2} g(N, T) [N_p(t) - N_0]. \quad (3)$$

$N_0$  is the carrier number at transparency,  $\tau_p$  is the photon lifetime,  $\tau_n$  is the carrier lifetime,  $\Gamma$  is the optical confinement factor describing the confinement mode in the active region,  $\beta$  is the spontaneous emission factor,  $\varepsilon$  is the gain compression factor,  $g(N, T)$  is the optical gain coefficient dependent on the carrier density and the temperature function,  $I(t)$  is the injected current,  $\alpha_0$  is the linewidth enhancement factor and  $q$  is the electron charge. The output power and the threshold current are given by: [7].

$$P(t) = \frac{\eta h \nu}{\tau_f} S_p(t) \quad (4)$$

$$I_{th} = \frac{q}{\tau_n} \left\{ n_0 + \frac{1}{g_0 \tau_p} \right\} \quad (5)$$

Where  $\eta$  is the quantum efficiency,  $h$  the Planck constant and  $\nu$  the radiation frequency. The steady-state solution to the rate equations is obtained by setting all the time derivatives  $\frac{dN_p(t)}{dt}$  and  $\frac{dS_p(t)}{dt}$  to zero. The carrier concentration that satisfies a given steady-state injected current is obtained by iterative self-consistent solutions of the two coupled equations. Hence, the couple rate equations (1) and (2) will be written as follow:

$$\frac{I(t)}{q} - \frac{N_p(t)}{\tau_n} - g(N, T) \frac{N_p(t) - N_0}{1 + \varepsilon S_p(t)} S_p(t) = 0 \quad (6)$$

$$\Gamma g(N, T) \frac{N_p(t) - N_0}{1 + \varepsilon S_p(t)} S_p(t) - \frac{S_p(t)}{\tau_p} + \Gamma \frac{\beta N_p(t)}{\tau_n} = 0 \quad (7)$$

Using equations (6) and (7) the carrier number  $N$  will be deduced as follow:

$$N = \frac{\frac{I(t)}{q \cdot V} - \frac{\tau_n S_p}{\tau_p \Gamma}}{\beta - 1} \quad (8)$$

## 3. Photon density S(f) and Frequency Response of the Semiconductor Laser.

### 3.1. Photon density

For laser with small signal, the expression of the photon density  $S(f)$  and transfer function  $R(f)$  above threshold are as follow [8].

$$R(f) = \frac{\text{photon Density}}{\text{Excitation Current}} = \frac{S_p(f)}{i(f)} = \frac{S_p(0)}{i(0)} \frac{f_0^2}{f_0^2 - f^2 + j f f_d} \quad (9)$$

Where:

$$f_0 = \frac{1}{2\pi} \sqrt{\frac{g_0 \eta}{\tau_p} (I - I_{th})} = \text{Resonance frequency} \quad (10)$$

$$f_d = \frac{\epsilon \eta (I - I_{th})}{2\pi \tau_p} = \text{Damping frequency} \quad (11)$$

$$f_p = \sqrt{f_0^2 - \frac{f_d^2}{4}} = \text{Frequency of peak response.} \quad (12)$$

### 3.2. Amplitude signal modulation

We consider a power modulation given by:

$$P(t) = P_0 [1 + M \cdot \cos(2\pi F_M t)] \quad (13)$$

where  $P_0$  is the unmodulated power and  $P(t)$  is the modulated power. The parameter  $M$  is called the power modulation index. The signal on the photodiode is modulated at a frequency  $F_m$ . At the output of the Fabry- Perot, we observe the optical spectrum. For weak  $M$ , the electric field can be written as follows: [9].

$$E_L(t) = A \left[ 1 + \frac{M}{2} \cdot \cos(2\pi f t) \right] \cdot \cos(2\pi \nu_L t + \phi_L) \quad (14)$$

$$E(t) = A \cos(2\pi \nu_L t + \phi_L) + M \frac{A}{4} \cos(2\pi(\nu_L - f)t + \phi_L) + M \frac{A}{4} \cos(2\pi(\nu_L + f)t + \phi_L) \quad (15)$$

### 3.3. Frequency signal modulation

Let us now consider a pure sinusoidal frequency modulation at frequency  $f$ :

$$v(t) = \nu_L + \Delta v \cdot \cos(2\pi f t) \quad (16)$$

The phase of the electric field is given by:

$$\int_0^t dt' v(t') = \nu_L t + \frac{\Delta v}{2\pi F_m} \sin(2\pi f t) \quad (17)$$

The electric field can therefore be expressed as follows:

$$E_L(t) = A \cdot \cos \left[ 2\pi \nu_L t + \frac{\Delta v}{f} \cdot \sin(2\pi f t + \phi_L) \right] \quad (18)$$

We define  $m = \frac{\Delta v}{f}$  as the frequency modulation index:

This field can be expanded in a sum of sinusoidal terms using Fourier techniques as follows:

$$E_L = A \cdot J_0 \cos(2\pi \nu_L t + \phi_L) - A \cdot J_1(m) \cdot \cos(2\pi(\nu_L - f)t + \phi_L) + A \cdot J_1(m) \cdot \cos(2\pi(\nu_L + f)t + \phi_L) + A \cdot J_2(m) \cdot \cos(2\pi(\nu_L - 2f)t + \phi_L) + A \cdot J_2(m) \cdot \cos(2\pi(\nu_L + 2f)t + \phi_L) - A \cdot J_3(m) \cdot \cos(2\pi(\nu_L - 3f)t + \phi_L) + A \cdot J_3(m) \cdot \cos(2\pi(\nu_L + 3f)t + \phi_L) - A \cdot J_4(m) \cdot \cos(2\pi(\nu_L - 4f)t + \phi_L) + A \cdot J_4(m) \cdot \cos(2\pi(\nu_L + 4f)t + \phi_L). \quad (19)$$

Frequency modulation is therefore characterized by the presence of sidebands at harmonics of the modulation frequency generated by Bessel function  $J_i(m)$  for  $i = 1, 2, 3 \dots$ . Bessel functions can evaluate to zero for specific values of the modulation index. For example,  $J_0(2.4) = 0$ : the optical carrier at  $\nu_L$  is suppressed for the modulation index equal to  $m=2.4$

## 4. Numerical Simulation and Results.

### 4.1 Steady state solution

A desired modulated laser signal can be generated by direct injection of the laser diode by an electric signal  $I(t)$  of suitable format. The carrier number  $N_p(t)$ , the photon density or optical signal  $S_p(t)$  will carry the same information as the modulating electric signal  $I(t)$  does. Therefore, in the absence of current modulation, the laser diode emits a constant-power monochromatic light. The current modulation induces a variation of the power and frequency of the beam. The deriving current of a modulated laser diode is the sum of two terms. The first term represents the bias current,  $I_b$ , which sets a value above the threshold level of the laser while the second term, which determines the modulation level, is noted  $I_m$ . Both currents are adjusted to achieve the desired variable power. Hence, the injection current  $I(t)$ , which is assumed to represent the modulating electrical signal is given as follow: [10].

$$I(t) = I_b + I_m f(t) \quad (20)$$

Where  $f(t)$  is a time function which describe the signal current format.

The ZnO laser diode is formed by phosphorus doping a very thin layer of n-ZnO wafer. The cleaved facets of the semiconductor ZnO active region serve as mirrors for the laser cavity figure.1. A recombination between the electrons of the n-junction with the holes of the p-junction is obtained by an electric current. Photons emitted into a mode of the waveguide will travel along the waveguide and be reflected several times in the mirrors. When the gain is higher than the losses of the cavity the laser starts to oscillate. The energy of the emitted photons is therefore approximately equal to the band gap energy of the semiconductor.

Using the laser parameters listed in Table 1, the threshold current for the modeled laser diode is 50mA. Together with a parasitic time-constant of 0.5 ns, a typical plot of the transient carrier density and photon number from the deterministic single-mode model is recorded on figure.2.

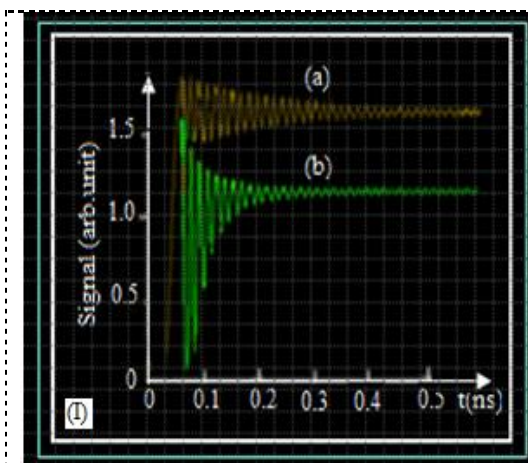
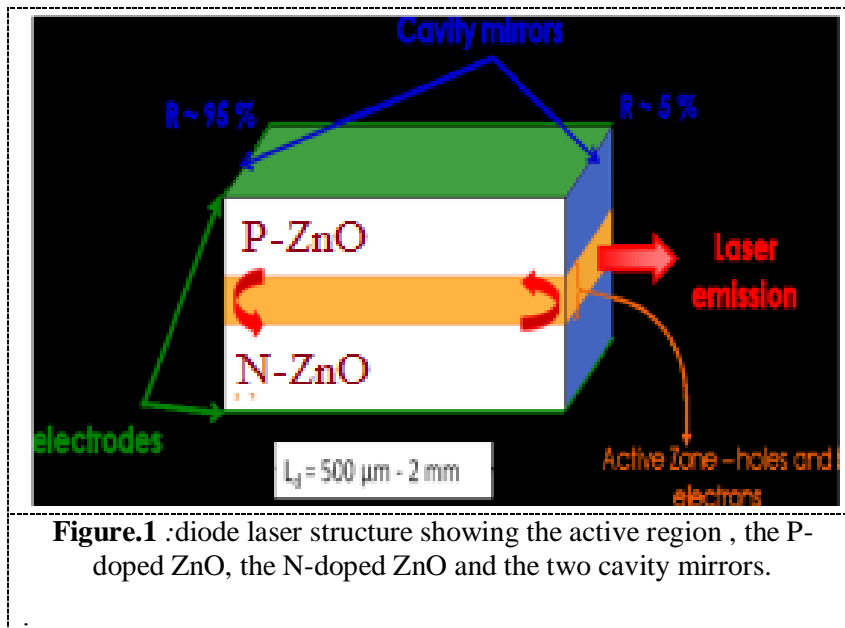
We note that the coupled relaxation oscillation occurs between the carrier density and photon number before reaching steady state.

The damping rate of laser relaxation oscillations is determined by the non linear gain and parasitic time-constant. As illustrated in figure.3a and figure.3b directly modulated lasers are derived by different value of the current source  $I(t)$ , which modulates the injected carrier density in the active layer.

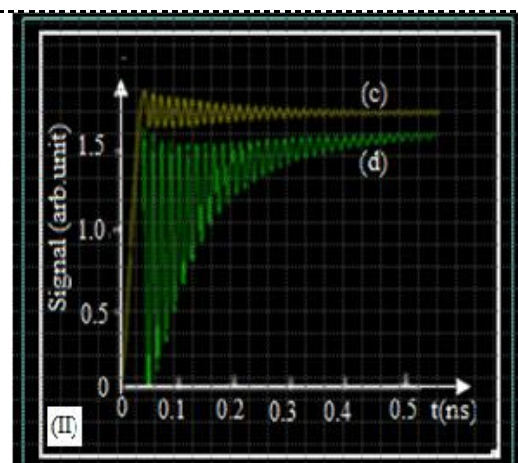
The laser operation and dynamics are influenced by property of gain suppression when the laser is biased above threshold, which originates from intraband relaxation processes of injected carriers. [11].

Table.1: diode laser parameters.

Parameter	Symbol	Value
Optical Confinement factor	$\Gamma$	0.05
Active region volume	$V$	$3 \cdot 10^{-11} \text{ cm}^3$
Spontaneous emission factor	$\beta$	$10^{-5}$
Photon Lifetime	$\tau_p$	$32 \cdot 10^{-12} \text{ s}$
Carrier lifetime	$\tau_n$	$2 \cdot 10^{-10} \text{ s}$
Slope gain constant	$g_0$	$5 \cdot 10^{-7} \text{ cm}^{-3} \text{ s}^{-1}$
Carrier density at transparency	$N_0$	$5 \cdot 10^{19} \text{ cm}^{-3}$
Quantum efficiency	$\eta$	0.5
Gain compression factor	$\epsilon$	$4 \cdot 10^{-17}$
Linewidth enhancement factor	$\alpha_o$	5



**Figure 2.I.** modulated laser derived by the current source  $I(t) = 40 \text{ mA}$



**Figure 2.II.** modulated laser derived by the current source  $I(t) = 30 \text{ mA}$

#### 4.2. Transient solution to the rate equations

To obtain transient solutions to the rate equations we have to solve numerically the rate equations to obtain the optical power and the phase of the electrical field at the laser output. For this, we use a fourth-order Runge-Kutta algorithm, we proceed first by a number of simplifying assumptions such as (1) the photon and electron distributions are spatially uniform, (2) the refraction index is spatially uniform and the effect of its variations with time is neglected, (3) the optical confinement factor and the spontaneous emission factor are treated as constant. [12].The computational result is given on figure.3

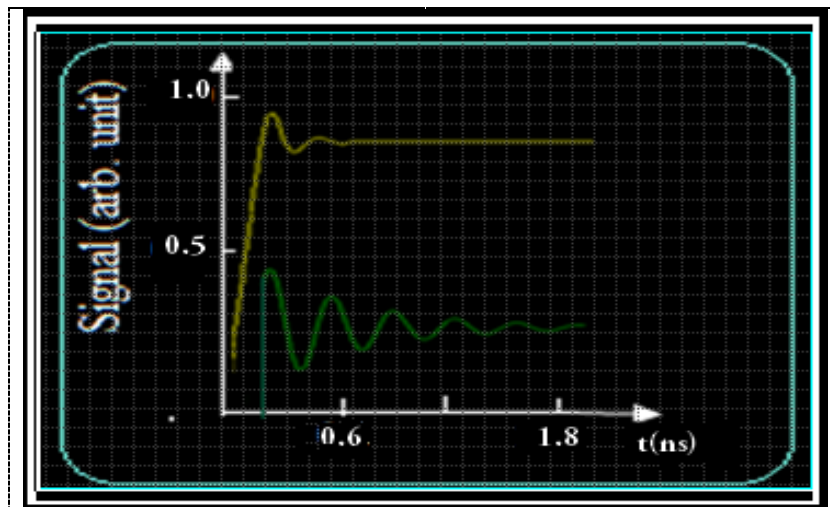


**Figure.3:** Transient dynamics of carrier density and photon number for a deterministic single mode rate-equation model with bias current of 50 mA.

It will be possible to obtain very short optical pulses, suitable for high-speed light wave telecommunication systems, from a quasi-rectangular modulation current. In these operation regime the small signal laser model, defining the modulation index as the ratio of the modulation current and the difference between the bias and the threshold current, we can obtain different pulses just by varying the bias current

In figure.4 we can see the simulated  $I(t)$  and the laser signal. It becomes clear that the optical signal can carry the same information as the modulating electric signal does. There exists a significant difference between the up and down levels of the optical signal such that one can distinguish the 1 and 0 bits. In addition, the bits duration of both the electric signals and the optical ones are identical.: [13].

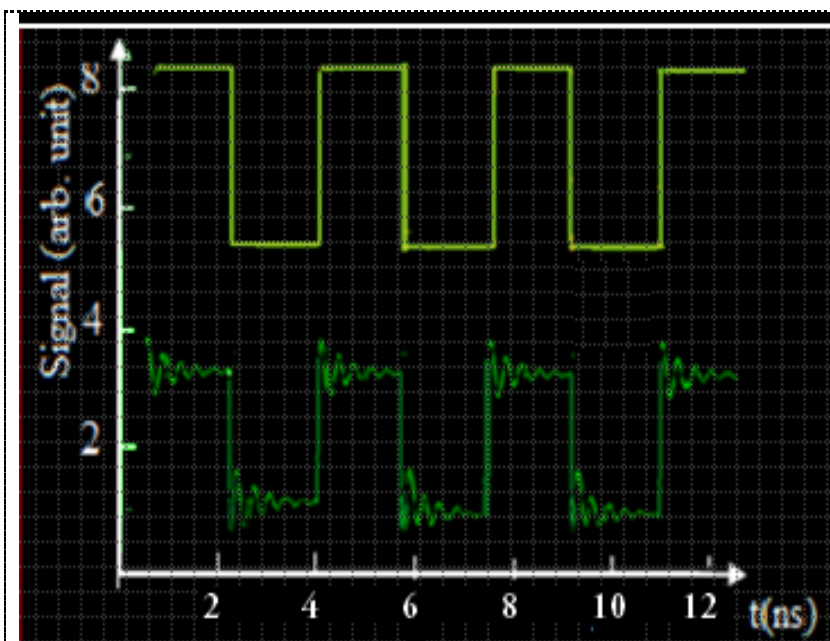


**Figure.4:** Transient dynamics of carrier density and photon number for a deterministic single mode suitable for high-speed light wave telecommunication systems.

### 4.3. Frequency response in optical modulation

In practice, optical modulation is a way to minimize the effects of electrical parasitics. Within the model, this is equivalent to adding an optical perturbation to optical signal generated by the carriers. The frequency response of the semiconductor laser, given by the equation 13, with the frequency response of the mount fixture.

On figure 5 we plot the simulated optical frequency responses of the laser obtained using the full model with parasite effects. We note that the bandwidth is mainly controlled by the resonance frequency figure.5 The damping due to the injected current variation is simulated and recorded on figure.6, the latter being significantly influenced by parasitics and adiabatic phenomenon. We note also that the bandwidth increases when the bias current increases [7,14].

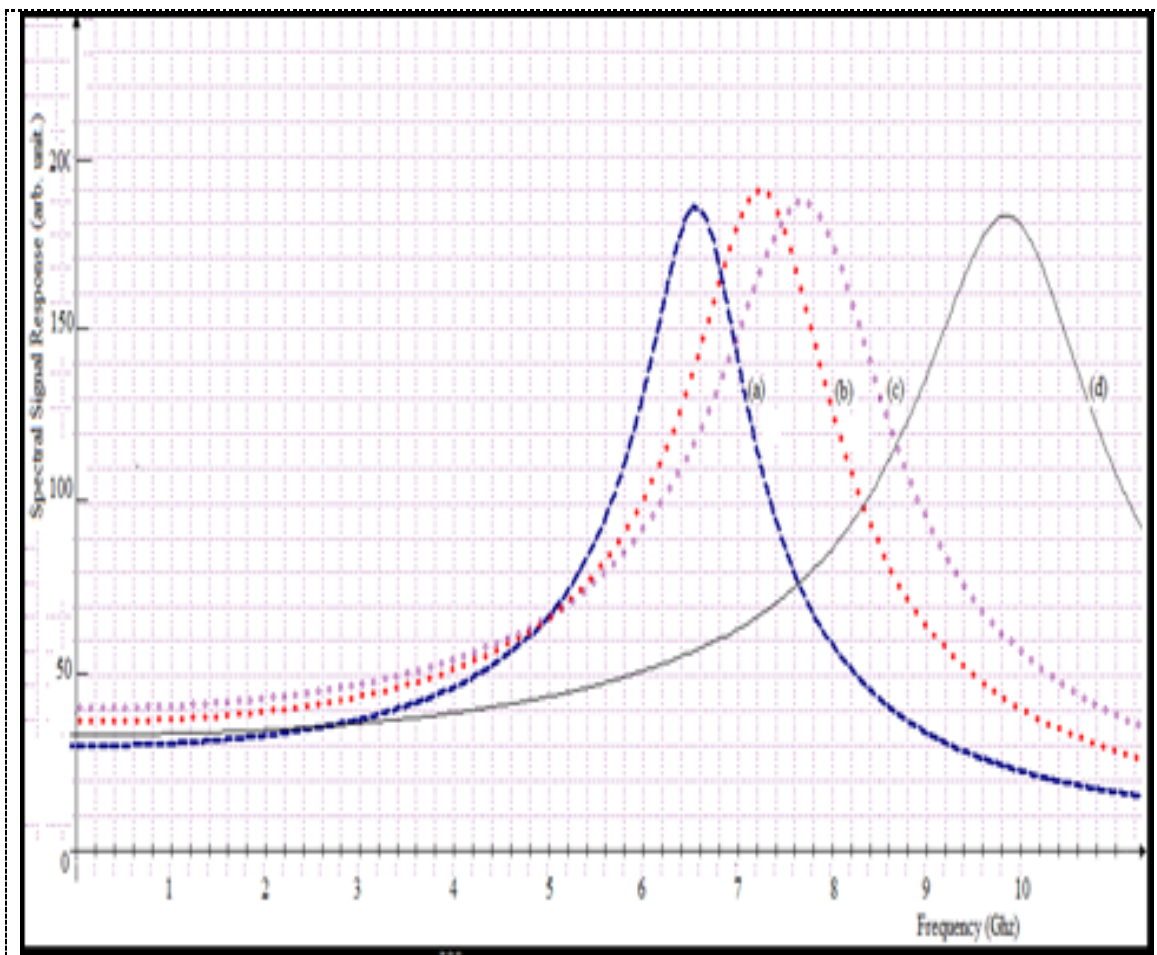


**Figure.5:** Variation of the bandwidth with the resonance frequency without damping  
a:  $f= 6.6$  GHz, b:7.4 GHz, c:7.8 GHz and d: 9.9 GHz.

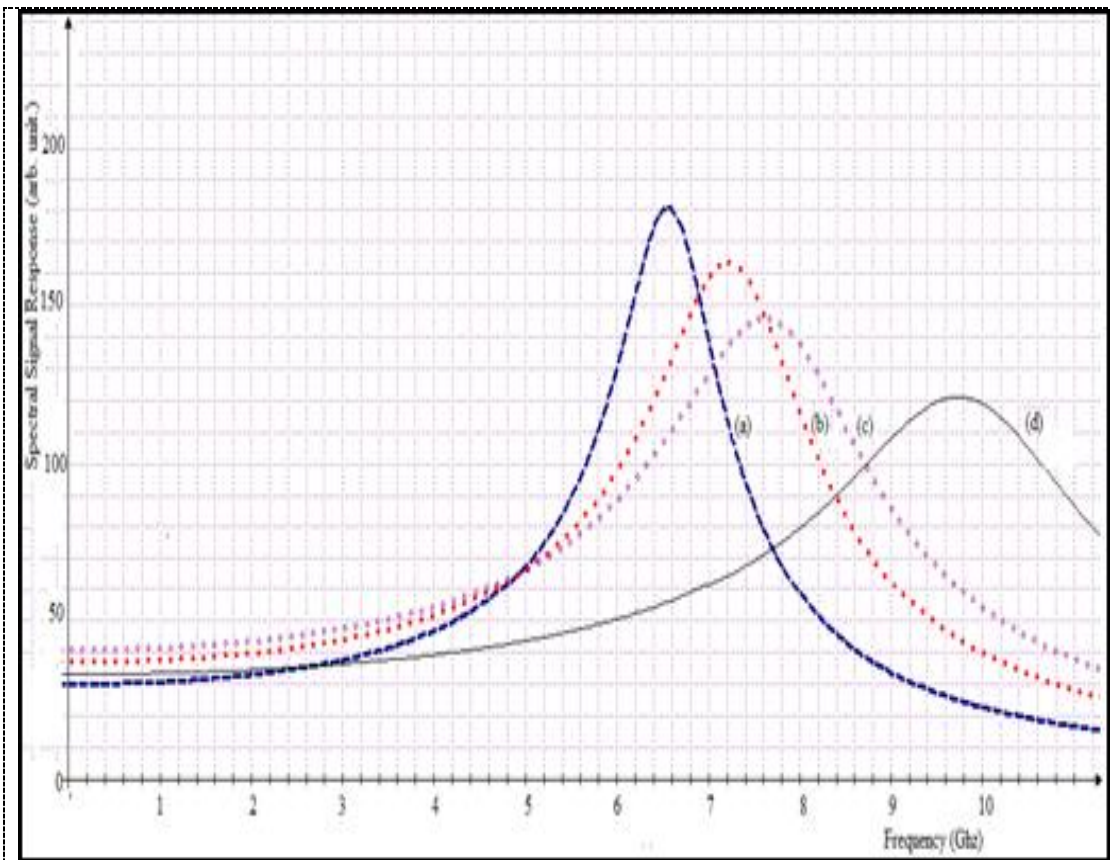


**Figure.6:** Variation of the bandwidth with the bias current  $I_b$   
 a:  $I_b = 30\mu\text{A}$ , b:  $I_b = 40\mu\text{A}$ , c:  $I_b = 50\mu\text{A}$  and d:  $I_b = 60\mu\text{A}$ .

We note (see figure 7-I) that the frequency curve bandwidth varies quasi-linearly with the material frequency response but its variation with the bias current, as showed on figure 7-II, does not seem one

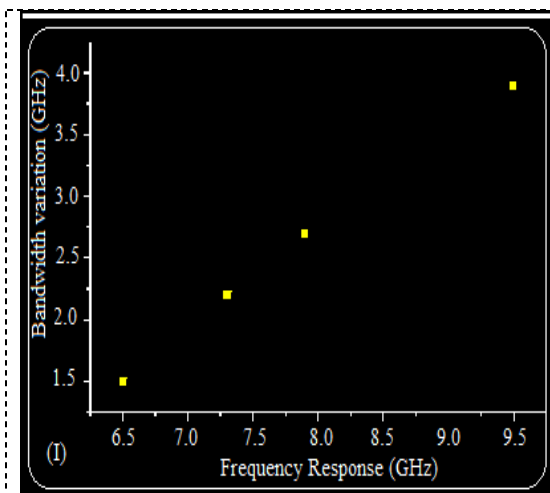


**Figure 7.I.** Bandwidth variation as function of frequency response.

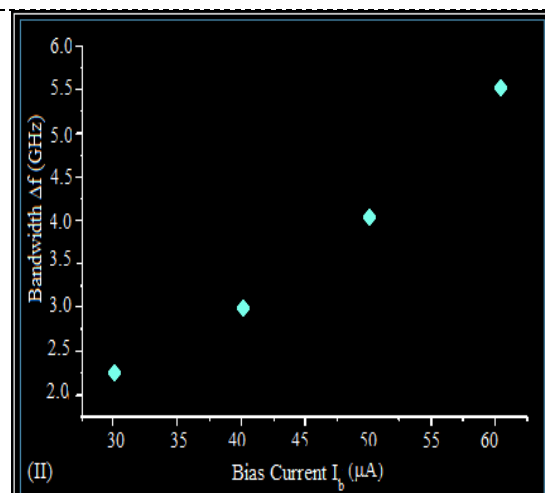


**Figure 7.II.** Bandwidth variation as function of the bias current.



#### 4.4. Frequency chirping

Diode lasers suffer from the frequency drift caused by changes in the junction temperature, by current noise, and by the perturbation of the external cavity length used for narrowing the laser spectrum. We can observe the effects of chirp on the spectrum of the signal modulated directly by amplitude modulation given by equation (15). This theoretical result is simulated and recorded on figure.8-I while the frequency modulation given by equation (19) is simulated and represented on figure.8-II.

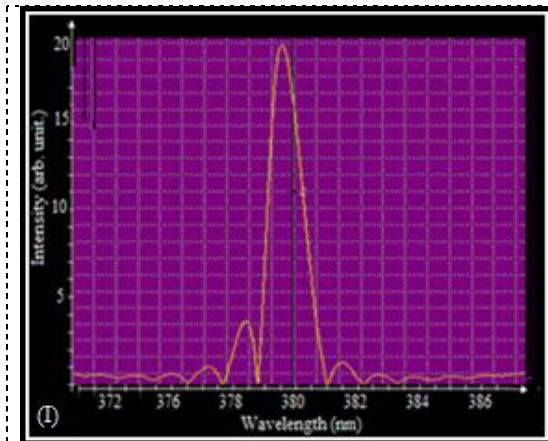


**Figure 8-I** Effects of chirp on the spectrum of the signal modulated directly by amplitude modulation.

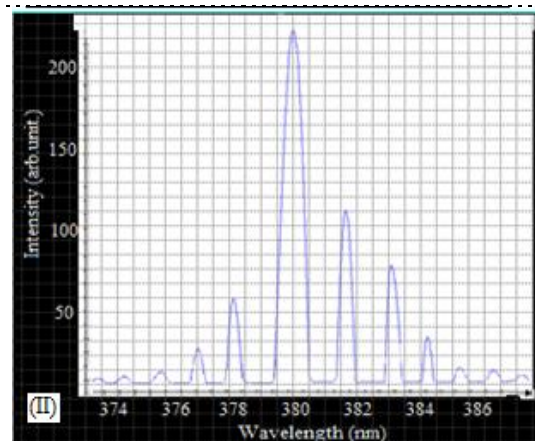


**Figure 8-II.** Effects of chirp on the spectrum of the signal modulated directly by frequency modulation.

The deformation of the carrier wave is the most visible effect occurring in the signal. This effect is quite larger at lower bit rates, as the adiabatic phenomenon is dominant. This is related to the transient chirp, and reveals that the frequency excursion, for the photon density, is different in minimum signal (low level) to the maximum signal (high level) figure.9[3]

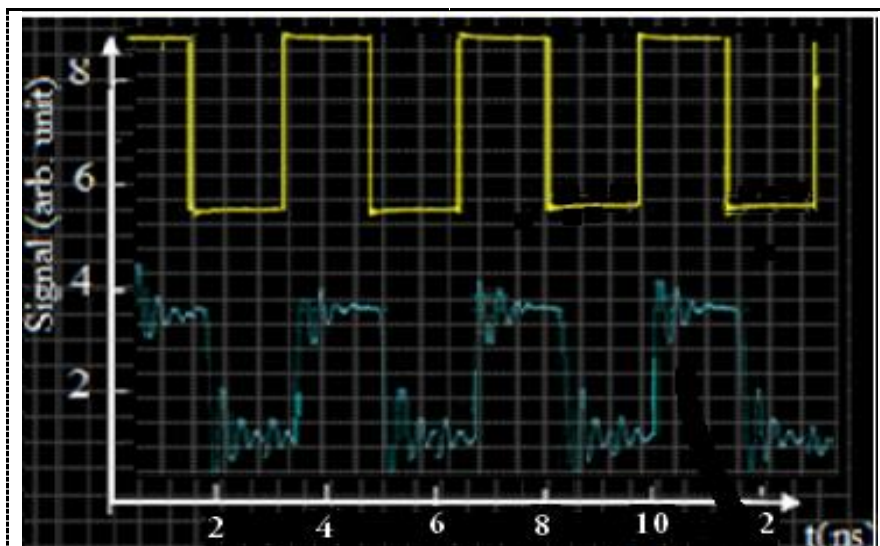


**Figure.9:** Frequency chirping visible on the single mode signal where the frequency excursion, for the photon density, is different in minimum signal (low level) compared to the maximum signal (high level).

## Conclusion

We have simulated a ZnO laser diode using an efficiency computational program and our results are in good agreement with others theoretical and experimental works. This program has been used to study the modulation response of laser diode emitting in the 380 nm ultraviolet wavelength. The simulation program developed can be used to illustrate the performance of a waveguide laser diode as function of device parameters for all semiconductors electrically pumped laser diode.

**Acknowledgement:** This work is supported by the PNR (National Research Program) Algiers (Algeria).

## References

- [1] R.A. Abdullah ,K. Ibrahim 2010 Optoelectronics and Advanced Materials–Rapid Communication **4** 568
- [2] Jeffrey O. White, George Rakulene, Carl Mungen 2011 ARL-TN0451 **1** 12
- [3] Safwat W.Z. Mahmoud 2007 Egypt Journal Solids **30** 277
- [4] M. Aleshams 2009 Progress In Electromagnetic Research **8** 121
- [5] H.K. Liang, S. F. Yu and H.Y. Yang (2010) Applied Physics letters **97** 241107
- [6] Matthew Lam, Ben Lunderwille, Matthew Von Schilling Applied Sciences 459 University of British Columbia
- [7] Vitezslav Jerabek, Ivan Huttel 2011 Radioengineering **20** 486
- [8] Linh V.T. Nguyen 2002 Systems Sciences Laboratory DSTO RR02
- [9] Krishna Myneni. Semiconductor 2011 Laser Rate Equation Solver 44 **1** 37
- [10] Thomas Erneux, Evgeny A. Viktorix and Paul Mandal 2007 Physical Review **A76** 0238
- [11] Ovidio H. Anton, Dinesh Patel Carmen S. Menoni, Jeng-Ya Yeh, T.T. Van Roy, L.J. Mawst, J.M.Pikal and Nelson Tansu 2005 Quantum Electronic **11** 1079
- [12] Asier Villafranca, Javier Lasobras and Ignacio Garcès Member, IEEE. TOYBA Lab. - I3A University of Zaragoza, PT Walqa, Ed. 1 22197 30 Janv-2Fev 2007 6th Spanish Conference on Electronic Devices
- [13] Sheng Chu, Guoping Wang , Weihang Zhou, Yuqing Kong, Lin Li, Jingjian Ren and Jianlin Liu 2011 Nature Technology Doi:10.1038 **6** 506
- [14] Sheng Chu ,Mario Olmedo, Zheng Yang , Jiaying Kong and Jianlin Liu 2008 Applied Physics Letters **93** 181106